Science and Technology Infusion Climate Bulletin
NOAA's National Weather Service
40th NOAA Annual Climate Diagnostics and Prediction Workshop
Denver, CO, 26-29 October 2015

A Revised Real-Time Multivariate MJO Index

Ping Liu[1], Qin Zhang[2], Chidong Zhang[3], Yuejian Zhu[4], Marat Khairoutdinov[1], Hye-Mi Kim[1]
Courtney Schumacher[5], and Minghua Zhang[1]

[1]*School of Marine and Atmospheric Sciences, Stony Brook University*
[2]*Climate Prediction Center, NCEP/NOAA/NWS*
[3]*RSAMS, University of Miami*
[4]*Environmental Modeling Center, NCEP/NOAA/NWS*
[5]*Texas A&M University*

1. Introduction

The Madden-Julian Oscillation (MJO; Madden and Julian 1971; 1972) is a dominant mode of tropical atmospheric variability on intraseasonal time scales. To monitor the real-time MJO evolution in magnitude and phase, Wheeler and Hendon (2004) developed the all-season Real-time Multivariate MJO (RMM) index which has been widely used (*e.g.*, Gottschalck *et al.* 2010). The index has a notable weakness, however. Straub (2013) found that zonal winds play a dominant role while OLR is minor in the index. Consequently, the RMM has tremendous difficulty representing the convective initiation of the MJO.

2. Problematic normalization step

The RMM index consists of the first two leading EOF modes of combined anomalies of OLR, 850-hPa zonal wind (U850) and 200-hPa zonal wind (U200). Before combination, the anomalies are normalized by the globally averaged standard deviation (STD) of respective variable: 15.3 W m^{-2} for OLR, 1.8 m s^{-1} for U850, and 4.9 m s^{-1} for U200. Such normalization is close to the conventional approach of dividing the STD of each anomalous series. In contrast, the OLR becomes over dominant in the RMM index if a covariance approach is used. After a series of tests, we found that scaling only the OLR with 2 W m^{-2} would make the contributions more balanced to form the revised RMM (RMM-r).

3. Improvement of RMM-r

The balance is supported by the wavenumber-frequency power spectra for each field reconstructed from the RMM modes. The difference between RMM-r and RMM indicates that RMM-r enhances the OLR power by 40-80% at zonal wavenumbers 2-5 and produces slight changes at zonal wavenumber 1 (Fig. 1a) and reduces power by about 20% in U850 (Fig. 1b), but only 10% in U200 (Fig. 1c).

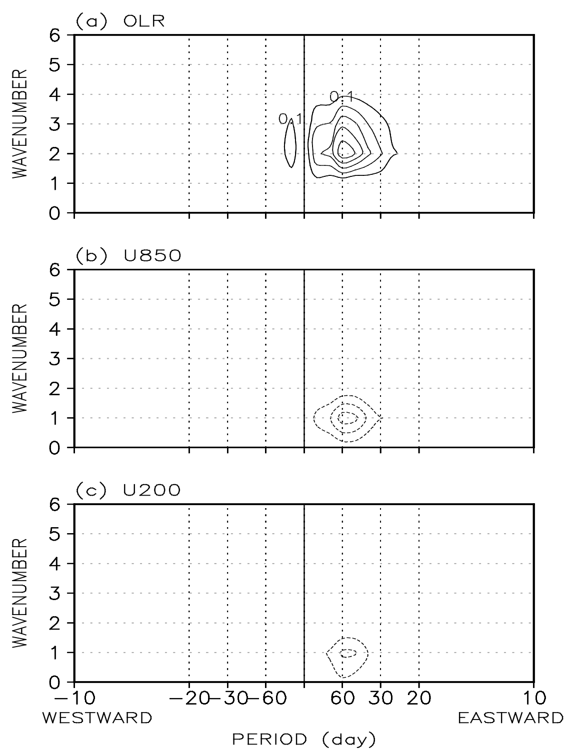

Fig. 1 Differences between the RMM-r and RMM in wavenumber-frequency power spectrum of anomalies reconstructed by the first two CEOF modes. One isoline in each is approximately equivalent to 7%, 11%, and 10%.

The improvement can be seen in representing the two TOGA-COARE MJO events (Webster and Luckas 1992). The first event is evident on the Hovmöller diagrams of OLR in raw (color shading in Fig. 2a) and total filtered

Correspondence to: Ping Liu, Endeavor Hall 199, School of Marine and Atmospheric Sciences, Stony Brook University, Stony Brook, NY 11794-5000; E-mail: Ping.Liu@stonybrook.edu.

MJO (contours in Figs. 2a, 2c, and 2d). It started near the end of November 1992 in the Western Indian Ocean. A large dry patch was then embedded in the evolution for about 10 days between 6 and 16 December, causing the wet band to be very narrow. This patch disappeared in the filtered MJO. After this patch, a wet phase redeveloped in the Western Pacific and peaked at about 170°E with a magnitude of -50 ~ -70 W m^{-2} in raw OLR while the corresponding value was less than half in the filtered MJO (only two contours). The second event was initiated over Africa and followed immediately the first event. It had two peak phases in raw OLR: one in the Central Indian Ocean with a magnitude smaller than -60 W m^{-2}, and the other near the dateline of about -60 W m^{-2}.

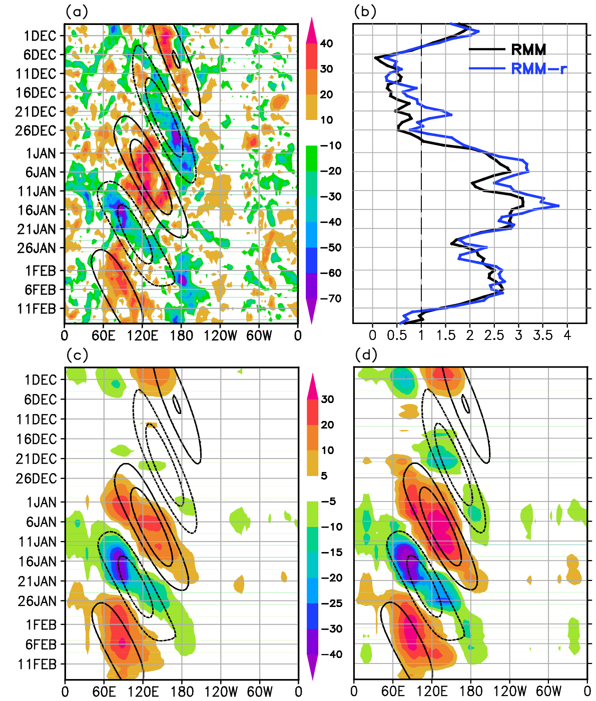

Fig. 2 The two TOGA-CORE MJO events for (a) raw OLR anomaly (shading) and filtered MJO (contour with interal 10 W m^{-2} and 0 being omitted); (b) amplitudes of RMM (black) and RMM-r (blue); (c) reconstructed anomalies (shading with uneven intervals) by RMM and total filtered MJO (contour as in a); and (d) same as (c) but by RMM-r.

The amplitudes in RMM and RMM-r overall capture both events from their initiation to peak phases (Fig. 2b), while notable changes were made by RMM-r during the first event. The RMM-r amplitude becomes above 1 again on 18 December, which is about one week earlier than RMM. Between 16 and 25 December, the RMM-r amplitude is nearly twice much as RMM, more consistent with the evolution and magnitude of the peak around 21 December on the Hovmöller diagram (*cf.* Fig. 2a). For the second MJO event, RMM-r has two peaks on 5 and 15 January 1993 and they are about 20-40% larger than the RMM peaks, which is more consistent with the Hovmöller diagram as well.

The reconstructed OLR amplitudes are improved as on Hovmöller diagrams (Figs. 2c and 2d). For the first event, RMM-r (Fig. 2d) has a much larger magnitude than RMM (Fig. 2c), and the duration of the suppressed phase before the redevelopment is much shorter. For the second event, the reconstructed OLR between 110°E and the date line is about 10-20 W m^{-2} smaller in RMM-r (Fig. 2d) than in RMM (Fig. 2c), suggesting stronger convection in RMM-r and closer to the raw and filtered MJO in Fig. 2a.

The improvement can be demonstrated on the RMM phase diagram too. For the first TOGA-CORE event (Fig. 3a), RMM-r (blue curve) detects it starting over the Western Indian Ocean in Phase 2, which is more eastward than RMM (black curve) in Phase 1 as shown by the different locations of the two black dots. The RMM-r remains outside of the unit circle for a few days and enters the circle at the Central Indian Ocean, also more eastward and with larger amplitude than the RMM. Later, the RMM-r emerges out of the circle in Phase 5 slightly to the east of the Maritime Continent and remains strong for several days towards the end in Phase 6 corresponding to the MJO redevelopment (*cf.* Fig. 2a). This phase evolution of RMM-r is also in a better agreement with the raw OLR than that

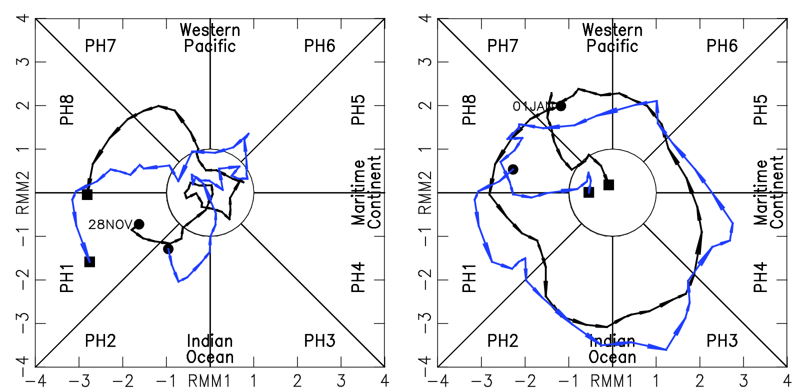

Fig. 3 Catesian phase diagrams of RMM (black) and RMM-r (blue) for the two events during TOGA-CORE (a) 28 November 1992 - 5 January 1993 and (b) 1 January - 15 Febrary 1993.

of RMM. The enhanced OLR variance in RMM-r obviously contributes to the change (*cf.* Fig. 2). For the second event during TOGA-CORE, both RMM and RMM-r represent its evolution well (Fig. 3b). There are still a couple of notable changes in the RMM-r. It peaks in Phases 3 over the Eastern Indian Ocean and Phase 4 over the Maritime Continent, while RMM peaks only once over the central Indian Ocean. The RMM-r amplitude is larger than RMM in Phases 1-5. Clearly RMM-r is more consistent with the actual MJO evolution.

This work has been published in *Monthly Weather Review* in 2016.

References

Gottschalck, J. and Coauthors, 2010: A framework for assessing operational Madden-Julian Oscillation forecasts: A CLIVAR MJO Working Group Project. *Bull. Amer. Meteor. Soc.*, **91**, 1247-1258.

Liu, P., Q. Zhang, C. Zhang, Y. Zhu, M. Khairoutdinov, H.-M. Kim, C. Schumacher, and M. Zhang, 2016: A revised real-time multivariate MJO index. *Mon. Wea. Rev.*, **144**, 627–642. doi: http://dx.doi.org/10.1175/MWR-D-15-0237.1

Madden, R. A., and P. R. Julian, 1971: Detection of a 40-50 day oscillation in the zonal wind in the tropical Pacific. *J. Atmos. Sci.*, **28**, 702-708.

Madden, R. A., and P. R. Julian, 1972: Description of global-scale circulation cells in the tropics with a 40-50 day period. *J. Atmos. Sci.*, **29**, 1109-1123.

Straub, K. H., 2013: MJO initiation in the Real-time Multivariate MJO index. *J. Climate*, **26**, 1130-1151.

Webster, P. J., and R. Lukas, 1992: TOGA COARE: the coupled ocean-atmosphere response experiment. *Bull. Amer. Meteor. Soc.*,**73**, 1377-1416.

Wheeler, M. C., and H. H. Hendon, 2004: An all-season Real-time Multivariate MJO index: Development of an index for monitoring and prediction. *Mon. Wea. Rev.*, **132**, 1917-1932.